The EMBO Journal (2011) 30, 2266–2280 | © 2011 European Molecular Biology Organization | All Rights Reserved 0261-4189/11
www.embojournal.org

THE EMBO JOURNAL

APP and APLP2 are essential at PNS and CNS synapses for transmission, spatial learning and LTP

This article has been corrected since Advance Online Publication and a corrigendum is also printed in this issue.

Sascha W Weyer[1,8], Maja Klevanski[1,8], Andrea Delekate[2,8], Vootele Voikar[3], Dorothee Aydin[1], Meike Hick[1], Mikhail Filippov[1], Natalia Drost[1], Kristin L Schaller[4], Martina Saar[1], Miriam A Vogt[5], Peter Gass[6], Ayan Samanta[7], Andres Jäschke[7], Martin Korte[2], David P Wolfer[3,6], John H Caldwell[4] and Ulrike C Müller[1,*]

[1]Department of Bioinformatics and Functional Genomics, Institute of Pharmacy and Molecular Biotechnology, Heidelberg University, Heidelberg, Germany, [2]Cellular Neurobiology, Zoological Institute, TU Braunschweig, Braunschweig, Germany, [3]Institute of Anatomy and Zurich Center for Integrative Human Physiology, University of Zurich, Zurich, Switzerland, [4]Department of Cell and Developmental Biology, Institute of Physiology and Biophysics, University of Colorado School of Medicine, Aurora, CO, USA, [5]Department for Psychiatry and Psychotherapy, Central Institute of Mental Health, Mannheim, Germany, [6]Department of Biology, Institute of Human Movement Sciences, ETH Zurich, Zurich, Switzerland and [7]Department of Pharmaceutical Chemistry, Institute of Pharmacy and Molecular Biotechnology, Heidelberg University, Heidelberg, Germany

Despite its key role in Alzheimer pathogenesis, the physiological function(s) of the amyloid precursor protein (APP) and its proteolytic fragments are still poorly understood. Previously, we generated APPsα knock-in (KI) mice expressing solely the secreted ectodomain APPsα. Here, we generated double mutants (APPsα-DM) by crossing APPsα-KI mice onto an APLP2-deficient background and show that APPsα rescues the postnatal lethality of the majority of APP/APLP2 double knockout mice. Surviving APPsα-DM mice exhibited impaired neuromuscular transmission, with reductions in quantal content, readily releasable pool, and ability to sustain vesicle release that resulted in muscular weakness. We show that these defects may be due to loss of an APP/Mint2/Munc18 complex. Moreover, APPsα-DM muscle showed fragmented postsynaptic specializations, suggesting impaired postnatal synaptic maturation and/or maintenance. Despite normal CNS morphology and unaltered basal synaptic transmission, young APPsα-DM mice already showed pronounced hippocampal dysfunction, impaired spatial learning and a deficit in LTP that could be rescued by $GABA_A$ receptor inhibition. Collectively, our data show that APLP2 and APP are synergistically required to mediate neuromuscular transmission, spatial learning and synaptic plasticity.

The EMBO Journal (2011) **30,** 2266–2280. doi:10.1038/emboj.2011.119; Published online 26 April 2011
Subject Categories: neuroscience; molecular biology of disease
Keywords: Alzheimer; amyloid precursor protein; knockout; learning; synaptic plasticity

Introduction

Synaptic dysfunction, cognitive decline, and deposition of the β-amyloid peptide Aβ, derived by proteolytic processing from the amyloid precursor protein (APP), are hallmark features of Alzheimer's disease (AD). Despite biochemical and genetic evidence that put Aβ as a central trigger for AD pathogenesis, the physiological role of APP and the question of whether a loss of its functions contributes to AD are still unclear. Interestingly, the neuroprotective secreted ectodomain APPsα is reduced in both familial and sporadic AD (e.g. Lannfelt *et al*, 1995; and references in Ring *et al* (2007)) and loss of APPsα-mediated functions may thus contribute to AD pathogenesis. Thus, it is essential to elucidate the *in vivo* function(s) of APP and its various proteolytic fragments, including their roles for synapse formation and function, as well as learning and memory.

APP processing is initiated by α-secretase cleavage within the Aβ region or by β-secretase (BACE) cleavage at the N-terminus of Aβ, leading to the secretion of large soluble ectodomains, termed APPsα and APPsβ, respectively. Subsequent processing by γ-secretase generates Aβ and the APP intracellular domain (AICD).

APP belongs to a gene family including the amyloid precursor-like proteins, APLP1 and APLP2, in mammals (Anliker and Müller, 2006). Although APLP1 and APLP2 lack the Aβ region, they are similarly processed by α-, β-, and γ-secretases (Walsh *et al*, 2007). APP and APLP2 are highly expressed in neurons and peripheral tissue including skeletal muscle, are axonally transported (Szodorai *et al*, 2009), and have been localized to peripheral neuromuscular junction (NMJ) and central synapses.

Our analysis of APP knockout (KO) mice revealed deficits in body and brain weight, a deficit in grip strength and in aged mice also impairments in learning and memory associated with a deficit in LTP (Ring *et al*, 2007). Combined knockouts indicated functional complementation within the APP gene family and revealed a key physiological role of APLP2. Indeed, $APP^{-/-}APLP1^{-/-}$ mice are viable, whereas

*Corresponding author. Department of Bioinformatics and Functional Genomics, Institute of Pharmacy and Molecular Biotechnology, Heidelberg University, Im Neuenheimer Feld 364, Heidelberg 69120, Germany. Tel.: +49 622 154 6717; Fax: +49 662 154 5830; E-mail: u.mueller@urz.uni-hd.de
[8]These authors contributed equally to this work

Received: 20 January 2011; accepted: 16 March 2011; published online: 26 April 2011; corrected: 12 May 2011

$APP^{-/-}APLP2^{-/-}$ and $APLP1^{-/-}APLP2^{-/-}$ mice die within 24 h after birth, likely due to impaired neuromuscular transmission (Heber *et al*, 2000; Herms *et al*, 2004; Wang *et al*, 2005). Whereas brain morphology of newborn double mutants was normal, triple KO mice showed cortical neuronal ectopias, indicating a role of the APP family for neuronal positioning (Herms *et al*, 2004). At the NMJ, APP and APLP2 have a redundant and essential role for synapse formation and function, as APP/APLP2 double knockout (DKO) mice exhibit widening of the endplate band and severely impaired neurotransmission (Wang *et al*, 2005). More recently, a study with selective gene knockout either in nerve or in muscle suggested a requirement of APP/APLP2 at both pre- and post-synaptic sites (Wang *et al*, 2009). Nonetheless, a detailed understanding of the specific function(s) of APP family members at the synapse and the role of the various proteolytic fragments remain unclear.

Knockout of the *C. elegans* orthologue APL-1 disrupts molting and morphogenesis and results in larval lethality. Interestingly, this lethality could be rescued by neuronal expression of the secreted extracellular domain (Hornsten *et al*, 2007). To dissect domains important for APP function in mice, we previously generated APPsα knock-in (KI) mice expressing only secreted APPsα. When compared with completely APP-deficient animals, APPsα-KI mice displayed a wild-type-like phenotype suggesting that APPsα (similar to secreted APL-1) is sufficient to rescue all abnormalities previously observed in adult APP-KO animals (Ring *et al*, 2007). Surprisingly, however, recently generated APPsβ-KI mice proved unable to rescue the perinatal lethality of APP/APLP2-DKO mice (Li *et al*, 2010), raising the question whether different secreted APP fragments may perform distinct functions.

Until now, the perinatal lethality of APP/APLP2-DKO precluded the analysis of APP/APLP2-mediated functions in the adult nervous system. To test whether APPsα, as opposed to APPsβ, may rescue the lethality and neuromuscular deficits of APP/APLP2-DKO mice, we crossed APPsα-KI mice onto an APLP2-deficient background. The majority of these APPsα-DM mice survive into adulthood revealing a complex phenotype with deficits both in synaptic transmission in the adult PNS and CNS and in learning and memory.

Results

Viable APPsα-DM mice show muscular weakness and deficits in challenging neuromotor tasks

In APPsα-KI mice, we inserted a stop codon behind the α-secretase cleavage site of the endogenous APP locus. Thus, APPsα-KI mice express only secreted APPsα (Supplementary Figure S1A). To test whether the apparent absence of phenotypic abnormalities in APPsα mice is due to functional complementation by APLP2, we crossed APPsα-KI mice with APLP2-deficient mice. Resulting APPsα-DM double mutant mice were born at normal Mendelian frequencies (χ^2 $F(2) = 1.4056$ ns). Remarkably, about half of these combined APPsα-DM mutants survived into adulthood (Supplementary Figure S1B) showing a reduction in body weight (Supplementary Figure S1C). Thus, expression of APPsα was sufficient for rescuing to a large extent the lethality of APP/APLP2-DKO mice that die shortly after birth. This viability allowed us to assess postnatal functions mediated by APP and APLP2. We focused our analysis on the NMJ, hippocampal formation, and behavioural tests of learning and memory.

Previously, we had demonstrated a deficit in grip strength in adult APP-KO mice (Ring *et al*, 2007), whereas both APPsα-KI mice and APLP2-KO mice were normal. On the accelerating rotarod, that assesses motor coordination and muscle fatigue, APPsα-DM mice performed poorly, falling off much earlier than APLP2-KO controls (Figure 1A showing female mice and Supplementary Figure S8A for animals of both sexes). In addition, APPsα-DM mice exhibited pronounced muscular weakness in the grip strength test (Figure 1B; Supplementary Figure S8B). Whereas all control mice were able to hang for at least 60 s from an inverted cage lid, APPsα-DM mice fell off immediately or after a few seconds (Figure 1C; Supplementary Figure S8C). As a baseline for subsequent cognitive tests, we also assessed activity in the home cage and the open field (Supplementary Figure S2A–C). Basal activity in the home cage was increased (Supplementary Figure S2A). In the novel open field arena overall activity, velocity and acceleration were not reduced in APPsα-DM mice (Supplementary Figure S2B and C). These data indicate that in the absence of APLP2, APPsα is not

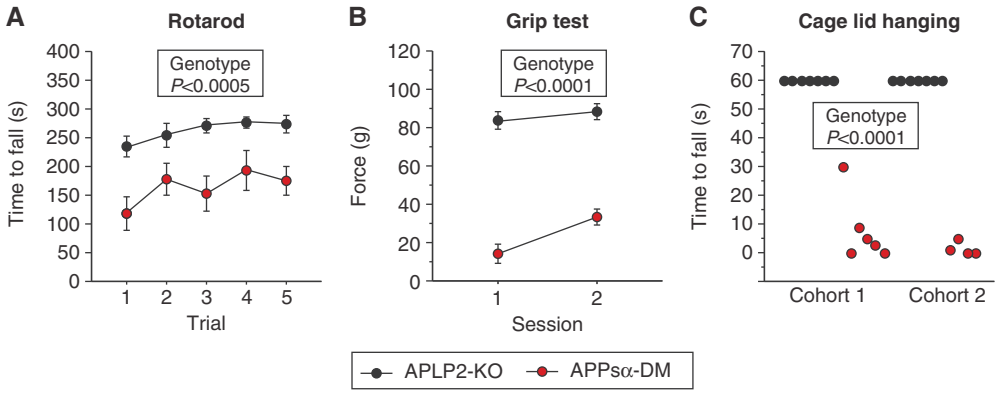

Figure 1 APPsα-DM mice show muscular weakness. (**A**) Rotarod testing. Time to fall during trials 1–5 of the accelerating rotarod test, max. time 300 s. APPsα-DM mice showed variable performance and were overall impaired (genotype $F(1,20) = 17.0$ $P < 0.0005$, trial $F(4,80) = 3.6$ $P < 0.0092$, trial × genotype $F(4,80) = 0.5$ ns). APPsα-DM $n = 10$, APLP2-KO $n = 14$, all female. (**B**) Grip test. Average grip force during two 5-trial testing sessions. APPsα-DM mice were strongly impaired (genotype $F(1,20) = 168.6$ $P < 0.0001$, session $F(1,20) = 8.5$ $P < 0.0086$, session × genotype $F(1,20) = 2.2$ ns). APPsα-DM $n = 10$, APLP2-KO $n = 14$, all female. (**C**) Cage lid hang test. APPsα-DM mice were strongly impaired (Mann–Whitney genotype $U = 140$ $P < 0.0001$). APPsα-DM $n = 10$, APLP2-KO $n = 14$, all female.

sufficient to mediate motor function needed for sustained high contraction forces, while basal locomotion is not impaired.

Impaired neuromuscular transmission: reduction in quantal content, readily releasable pool, and ability to sustain vesicle release

To examine whether the muscle weakness of APPsα-DM mice is a consequence of impaired NMJ function, we first studied spontaneous synaptic transmission. Miniature endplate potential (MEPP) frequency in both APLP2-KO and APPsα-DM muscle fibres was in the normal range of 0.5–1/s (Figure 2A). However, the distribution of frequencies was sharply altered in the APPsα-DM fibres with a high proportion of fibres showing very low frequency responses and some fibres with higher than normal MEPP frequencies (3–5/s; Figure 2B). Overall, this resulted in a significant decrease of mean MEPP frequency in double mutants (Figure 2A). Mean MEPP amplitudes, however, were increased by about 29% in APPsα-DM mice (Figure 2C), possibly due to post-synaptic changes that were not investigated in more detail. Evoked responses were recorded to study a potential defect in transmitter release. Single action potentials in the pre-synaptic axon produce the coordinated exocytosis of 50–100 synaptic vesicles (termed quantal content). We observed a dramatic reduction (by 45%) in quantal content in APPsα-DM muscles (29 ± 1.7) compared with APLP2-KO littermate control muscles (52.9 ± 3.3; Figure 2D; Supplementary Figure S3C). Short-term synaptic plasticity, assessed by paired-pulse-facilitation (PPF), was not significantly different (Supplementary Figure S3A and B).

The reduced quantal content could be due to a smaller readily releasable pool (RRP) and/or a smaller probability of release. The APLP2-KO muscle had a greater initial quantal content (Figure 2D) and released ~2.5-fold more vesicles during the 2 s stimulation (1610 versus 652; arrowheads in Supplementary Figure S3C). The RRP (determined according to Elmqvist and Quastel (1965)) in APPsα-DM muscles (298 ± 31) was about 30% of that of the APLP2-KO muscles (1004 ± 109; Figure 2E). Surprisingly, the probability of release from motoneurons (calculated as quantal content of the first response divided by the RRP) in the APPsα-DM muscles was twice as large as in the APLP2-KO muscles (0.1 versus 0.05; Figure 2F). Thus, the smaller quantal content in the APPsα-DM muscles was solely due to the reduction in RRP.

Since APPsα-DM mice are unable to maintain their grip upside down on a wire mesh (Figure 1C) for longer than 5–10 s, we stimulated the phrenic nerve for 10 s with either 20 or 40 Hz trains of action potentials (Figure 2G and H; Supplementary Figure S3D). Within the first second of stimulation, EPP size (normalized to the first response) in APPsα-DM muscles was ~20% smaller than in APLP2-KO muscles. A large deficit (15%) in APPsα-DM muscles was also observed for 40 Hz stimulation (Supplementary Figure S3D and E). Overall, these data suggest that neuromuscular weakness of APPsα-DM mice is likely due to both a reduction in quantal content, as well as impaired ability to maintain sustained transmitter release. Of note, this pre-synaptic defect in transmitter release seems to be specific for peripheral cholinergic neuromuscular synapses since no alterations in basal synaptic transmission or evoked pre-synaptic stimulation were detectable for glutamatergic CA3/CA1 excitatory synapses within the hippocampus (see Supplementary Figure S11B and C).

Mint2 binding to APP provides a link to Munc18-1

Our data suggest that holo-APP/APLP2 may be required for organizing the molecular complex for exocytosis and/or in positioning the release ready vesicles at the NMJ (Neher and Sakaba, 2008). In this regard, it is striking that Mint/X11 family members are known to bind the cytoplasmic domain of APP. Neuronal Mint1, 2 (X11α, β) both bind Munc18-1, which in turn binds the SNARE complex (Rogelj *et al*, 2006). Thus, we wondered whether members of the Mint/X11 family might link APP and Munc18-1. To test this hypothesis, we co-transfected HEK293 cells with APP, Mint2 and Munc18-1 and performed immunoprecipitations followed by western blotting (Figure 3A). Indeed, both Mint2 and APP could be co-immunoprecipitated with Munc18-1.

To explore the interaction of APP/Mint2/Munc18-1 in living cells, we employed the BiFC assay (Kerppola, 2008) by introducing APP-VC and Munc18-YN fusion proteins either alone or together with Mint2 (Figure 3B and C). As expected, expression of APP-VC together with Munc18-YN did not lead to an appreciable fluorescent BiFC signal in co-transfected cells. In contrast, significant fluorescence was detectable in triple-transfected cells expressing Mint2 in addition to APP-VC and Munc18-YN, suggesting that Mint2 serves as a scaffold that brings APP and Munc18-1 in close proximity. Importantly, formation of this tripartite complex critically depends on the APP C-terminus, as APPΔCT-VC constructs lacking the YENPTY interaction motive for Mint2, failed to yield fluorescence, despite readily detectable expression (as shown by immunocytochemistry) of transfected proteins (Figure 3C, middle).

APPsα-DM mice exhibit a widened endplate band

To assess whether deficits in synaptic transmission are associated with abnormal NMJ morphology, as seen in newborn DKO mutants (Wang *et al*, 2005), we studied the diaphragm from young adults (4 and 8 weeks of age). In APPsα-DM mice endplates visualized by bungarotoxin (BTX)-rhodamine staining appeared scattered and distributed over a much wider muscle territory, which was reflected by an increase in endplate band area of about 50% compared with APLP2-KO (Figure 4A–C). For quantification, the lateral distance and density of individual endplates from the medial tendon insertion was measured. When fitted with a Gaussian, the half-maximal width of the distribution in APPsα-DM muscle (450 ± 20 μm) was significantly increased by about 1.3-fold compared with muscles of APLP2-KO controls (346 ± 27 μm, $P < 0.05$, *t*-test; Figure 4C). Widening of the endplate band was paralleled by a pronounced increase in secondary nerve branching in APPsα-DM mice (Figure 4D). Although the precise branching pattern varies between individual mice, abnormalities were obvious in all mutants (data not shown).

APP/APLPs are necessary for NMJ synapse maturation and maintenance

Closer examination of synapses revealed several striking abnormalities in APPsα-DM mutants: (1) reduced size of pre- and post-synaptic specializations, (2) defective apposition of pre- and post-synaptic elements, and (3) abnormal topology of post-synaptic structures. In APPsα-DM mice, both

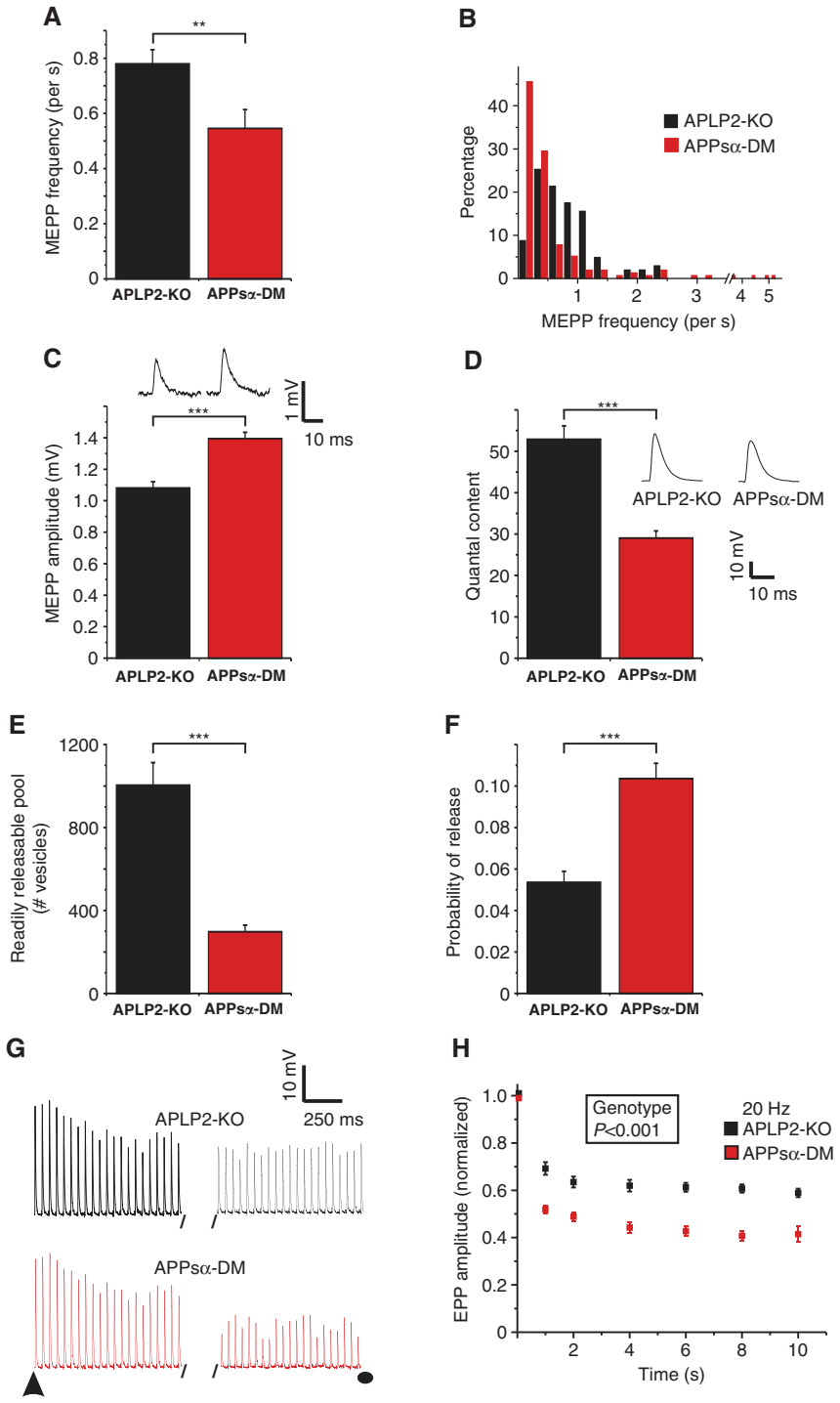

Figure 2 APPsα-DM mice show reduced quantal content, RRP and ability to sustain vesicle release. Spontaneous (**A–C**) and evoked (**D–H**) vesicle release recorded with intracellular recording in mouse diaphragm muscle fibres. (**A**) MEPP frequencies in APLP2-KO (black bar; freq = 0.78 ± 0.05/s, mean ± s.e.m.; 103 fibres, 9 muscles) and APPsα-DM (red bar; freq = 0.55 ± 0.07/s, s.e.m.; 155 fibres, 15 muscles) were significantly different ($^{**}P = 0.01$, *t*-test). (**B**) Distribution of MEPP frequency from fibres in panel (**A**). Note the large increase in fibres with low spontaneous release of vesicles in APPsα-DM. (**C**) MEPP amplitudes were significantly larger in APPsα-DM (1.39 ± 0.04 mV, s.e.m.) than in APLP2-KO fibres (1.08 ± 0.04 mV, s.e.m.; $^{***}P < 10^{-6}$, *t*-test). Same fibres and muscles as panel (**A**). (**D**) Quantal content (QC) during evoked release was over 80% larger in APLP2-KO fibres (QC = 52.9 ± 3.3, s.e.m.; 12 fibres, 3 muscles) than in APPsα-DM fibres (QC = 29 ± 1.7, s.e.m.; 45 fibres, 3 muscles; $^{***}P < 10^{-7}$). (**E**) Readily releasable pool (RRP) size in APPsα-DM was less than a third compared with APLP2-KO fibres. Mean RRP values for APLP2-KO (12 fibres, 3 muscles; RRP = 1004 ± 109, s.e.m.) and APPsα-DM (24 fibres, 3 muscles; RRP = 298 ± 31, s.e.m.; $^{***}P < 10^{-8}$). (**F**) Probability of release in APPsα-DM was double that of APLP2-KO fibres. Same synapses as panel (**E**). Calculated as the ratio of the quantal content of the first response of a train divided by the RRP of that synapse. APLP2-KO: 0.05 ± 0.005; APPsα-DM: 0.1 ± 0.007; $^{***}P < 10^{-4}$. (**G**, **H**) Decrease in evoked post-synaptic response during a 10 s, 20 Hz train of action potentials in the phrenic nerve. Responses during the first and last second are shown (stimulation continued during the 8 s gap). Arrowhead: start of stimulus, filled circle: end of stimulus. (**H**) Endplate potentials were measured at 1, 2, 4, 6, 8, and 10 s by averaging groups of five responses occurring during a 200-ms window. Amplitudes were normalized for APLP2-KO ($n = 12$ fibres, 3 muscles) and APPsα-DM ($n = 25$ fibres, 3 muscles). Error bars (s.e.m.) are smaller than the symbol for some data points. Differences at each time point (1–10 s) were statistically significant ($P < 10^{-3}$).

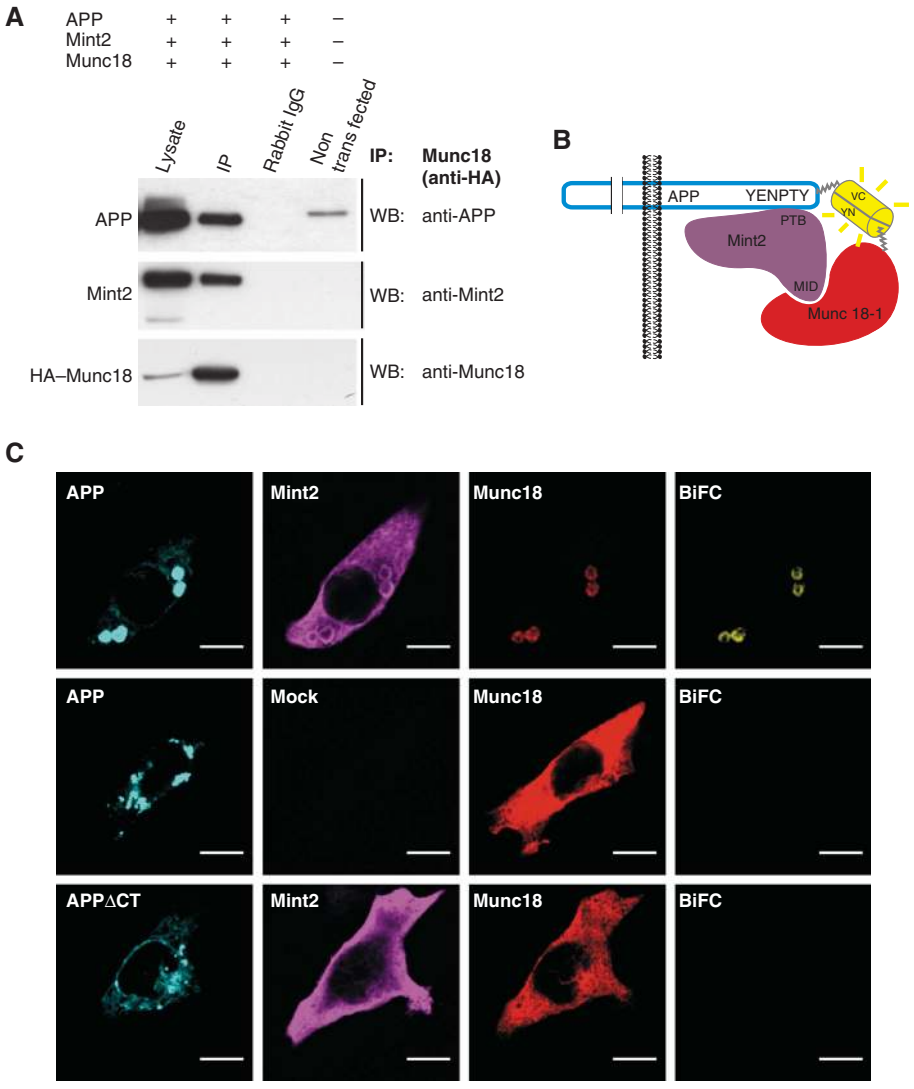

Figure 3 Interactions of APP with Mint2 and Munc18. (**A**) Immunoprecipitation and immunoblotting of HEK293 cells co-transfected with APP, Mint2, and HA-tagged Munc18-1. Cell lysates were immunoprecipitated with an anti-HA antibody (IP: Munc18, anti-HA) and probed with anti-APP (C1/6.1), anti-Mint or anti-Munc18 antibodies. IP with rabbit IgG served as a negative control. Lysate of non-transfected cells reveals endogenous APP. (**B**) Model of tripartite complex of APP-VC, Mint2 and Munc18-1-YN. (**C**) Visualization of the APP/Mint2/Munc18-1 complex by BiFC. Cos7 cells were co-transfected with YN-HA–Munc18 (all panels), mycAPP-VC (upper and middle panel) or mycAPPΔCT-VC (lower panel). In addition, co-transfections contained either Flag–Mint2 (upper and lower panel) or were mock transfected with pcDNA (middle panel). Expression was visualized by immunocytochemistry using anti-myc (for APP), anti-HA (for Munc18-1), and anti-mint antibodies. BiFC signal was imaged 24 h after transfection (scale bar: 10 μm).

the area covered by AChRs and the area of synaptophysin-immunoreactive pre-synaptic specializations were considerably reduced (Figure 5A–C). In addition, APPsα-DM revealed reduced coverage of the pre-synaptic marker synaptophysin with post-synaptic AChRs (Figure 5D). Interestingly, whereas all post-synaptic sites were innervated, we found in APPsα-DM animals several isolated synaptophysin-positive patches indicating pre-synaptic specializations that lacked any BTX staining (Figure 5E), suggesting either postnatal nerve terminal sprouting or more likely, persistence of pre-synaptic structures at sites at which post-synaptic specializations had been lost.

Intriguingly, whereas AChRs at APLP2-KO control NMJs (8 weeks of age) displayed a mature 'pretzel'-like pattern, with continuous and elaborately branched AChR clusters (Figure 5A), many endplates in APPsα-DM mutants appeared fragmented with AChRs arranged into numerous small discontinuous islands (Figure 5A and H). Quantification by either computer assisted image analysis (Figure 5F) or counting of fragments (data not shown) yielded an about two-fold increase in the mean degree of fragmentation for double mutants. Moreover, we noted a significant increase in the frequency of plaque-like endplates, a topology characteristic of neonatal NMJ (Figure 5G and H). These topological abnormalities could reflect a role of APP/APLP2 in the formation, maturation, or maintenance of NMJs. We, therefore, examined endplates from P21 to 28, a stage at which the early period of synapse elimination is complete (Sanes and Lichtman, 1999). At this stage, synaptic topology of double mutants was similar to APLP2-KO revealing no significant difference in the frequency of plaque-like or fragmented synapses (data not shown). Thus, these findings suggest that APP/APLP family members are important not only for synapse formation (as inferred from the widened endplate

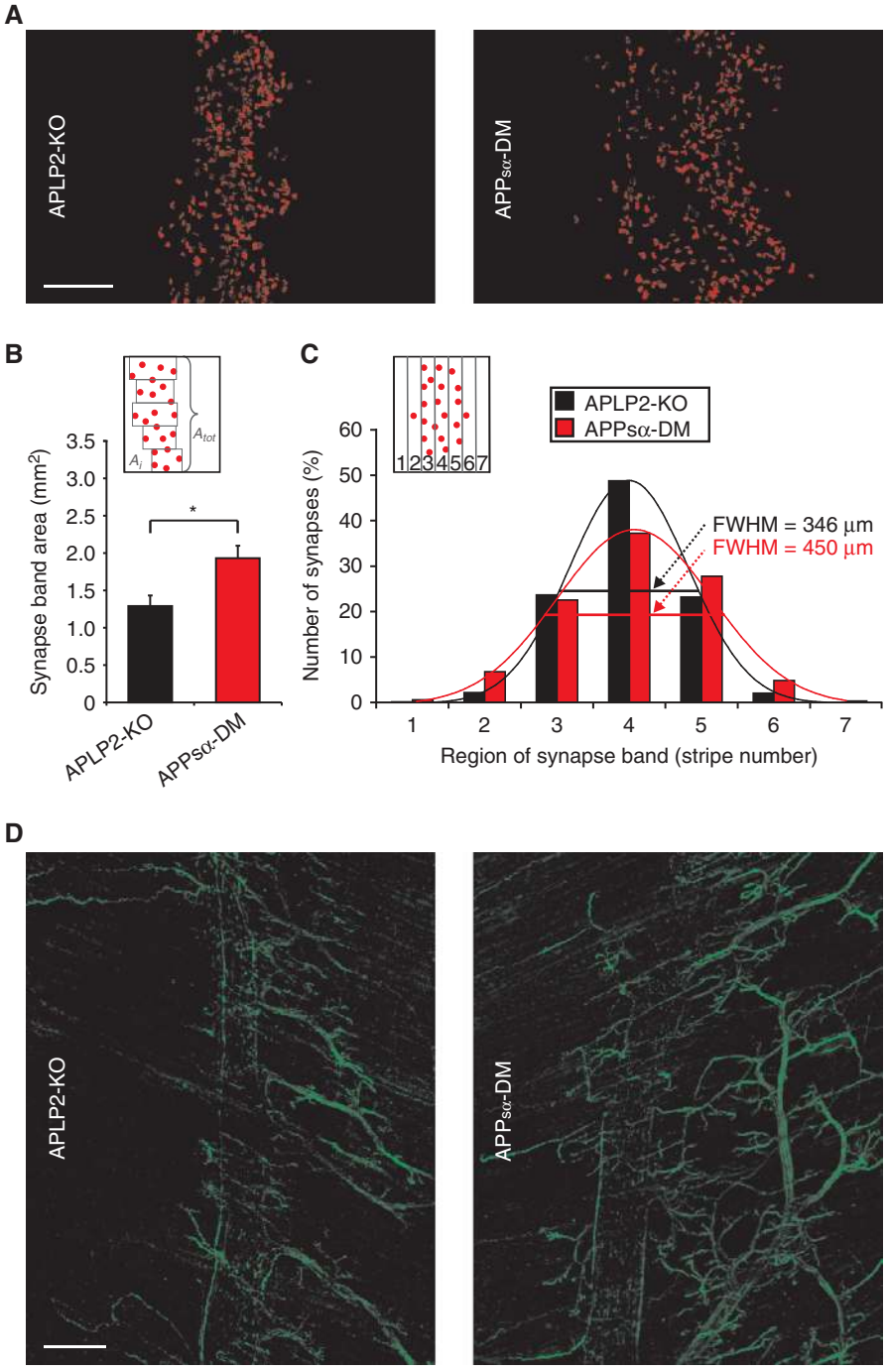

Figure 4 Widening of the endplate band in APPsα-DM mice. (**A**) Whole mount BTX staining of diaphragm. (**B**) Muscle area covered by AChR-rich synapses (height of microscopic field = 2485 µm). Values represent mean ± s.e.m.; mean number of synapses per mouse: APLP2-KO $n = 575$; APPsα-DM $n = 752$, $n = 3$ mice/genotype $^*P < 0.05$, *t*-test (age: 2 months). (**C**) % Synapses within seven stripes covering the synapse band. When fitted with a Gaussian the full width at half maximum (FWHM) of the synapse distribution is significantly increased in APPsα-DM ($P < 0.05$; *t*-test). (**D**) Neurofilament staining indicates increased branching of the phrenic nerve in APPsα-DM (age: 1 month). Scale bars: (**A**) = 250 µm and (**D**) = 150 µm.

band) but also in addition required for synapse maturation and/or maintenance. Muscle morphology of APPsα-DM diaphragm revealed no reduction in fibre number or fibre diameter, nor signs of fibre degeneration (absence of central myonuclei) excluding the possibility that defects in NMJ function and morphology were secondary to muscle damage (data not shown).

APPsα-DM mice reveal no alterations in hippocampal structure, neuronal morphology, and spine density of CA1 neurons

Histopathological analysis (as assessed by Nissl, Calbindin, Parvalbumin, and GFAP staining at 12 months) did not show any apparent abnormalities of cortical or hippocampal architecture in APPsα-DM compared with APLP2-KO

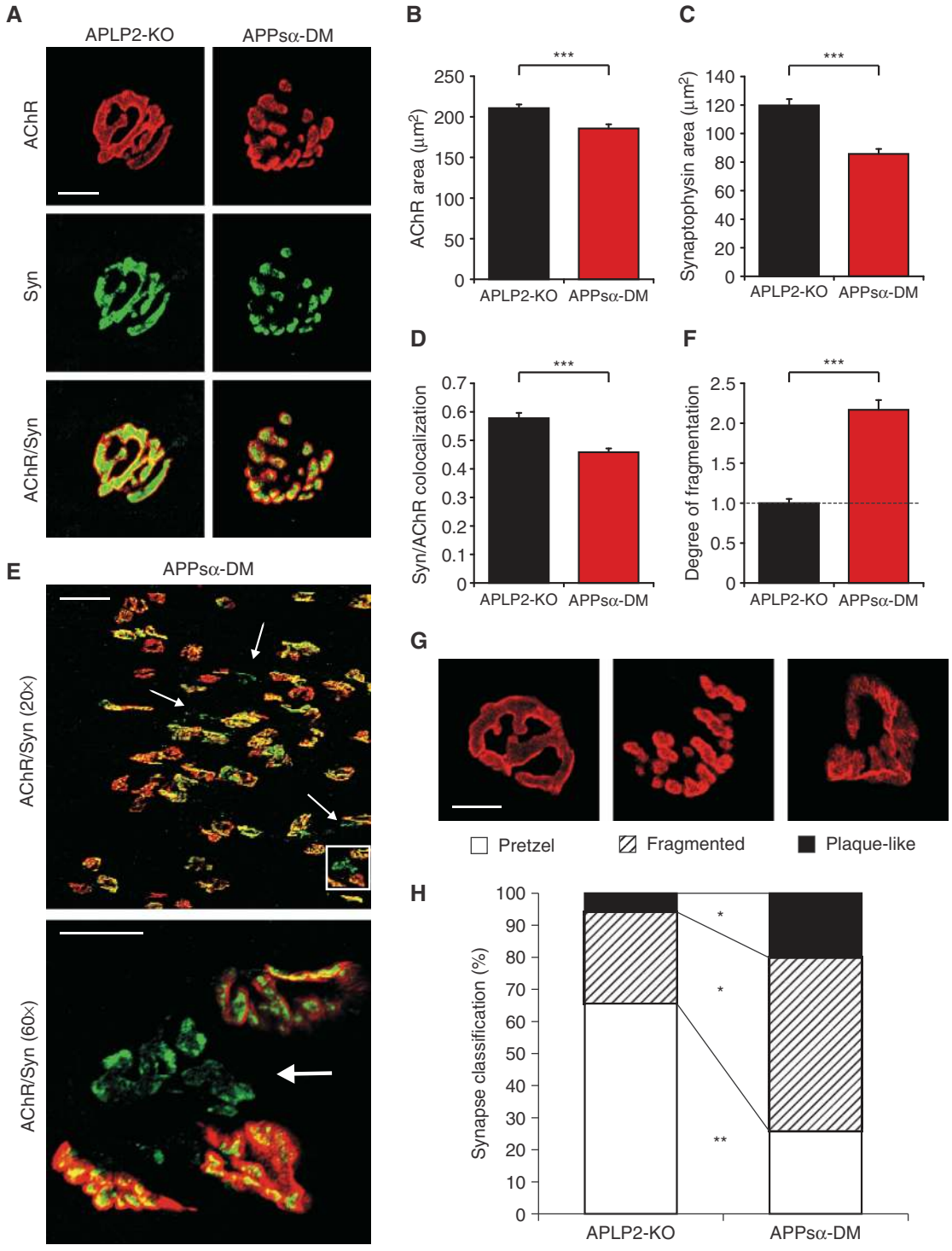

Figure 5 APPsα-DM mice show aberrant synaptic morphology and abnormal synaptic maturation. (**A**) In APPsα-DM synapses frequently show a fragmented structure with multiple discrete non-connected structures, APLP2-KO synapses were pretzel shaped. AChRs labelled by BTX (red), pre-synaptic terminals by anti-synaptophysin (Syn, green). (**B**) Synapse area covered by AChRs is significantly smaller in APPsα-DM mice. Number of synapses (**B**–**D**, **F**): APLP2-KO $n=109$, APPsα-DM $n=103$; 3 mice/genotype. (**C**) Synapse area occupied by synaptophysin is significantly smaller in APPsα-DM mice. (**D**) APPsα-DM mice showed reduced colocalization of pre- and post-synaptic structures compared with APLP2-KO. Colocalization ratio: synaptophysin area divided by AChR area. (**E**) APPsα-DM mice (age: 1 month) displayed multiple Syn^+ pre-synaptic structures not colocalized with AChRs (see arrows). Lower panel: higher magnification of boxed area. (**F**) Degree of fragmentation indicates the relative number of fragments per synapse, with values from APLP2-KO mice set as 1. APPsα-DM revealed a two times increased fragmentation index (see Materials and methods for details). (**G**) Synapses were classified into three categories. Pretzel class: synapses composed of 1–3 fragments (excluding plaque-like structures); fragmented synapses: composed of ≥4 fragments; plaque-like synapses: oval/half-moon shaped, lacking complex branching. Note also the lack of sharp contours with high AChR density. On average, 67 synapses were analysed per mouse, $n=3$ mice/genotype. (**H**) APLP2-KO mice revealed predominantly pretzel-like post-synaptic structures whereas APPsα-DM mice showed significantly more fragmented and plaque-like synapses (age (**G**, **H**): 2 months). For entire figure: Error bars reflect s.e.m. Asterisks denote unpaired *t*-test, $***P<0.001$ $**P<0.01$,$*P<0.05$. Scale bars: (**A**), $(\mathbf{E})_{\text{lower panel}}$, (**G**) = 10 μm; $(\mathbf{E})_{\text{upper panel}}$ = 50 μm.

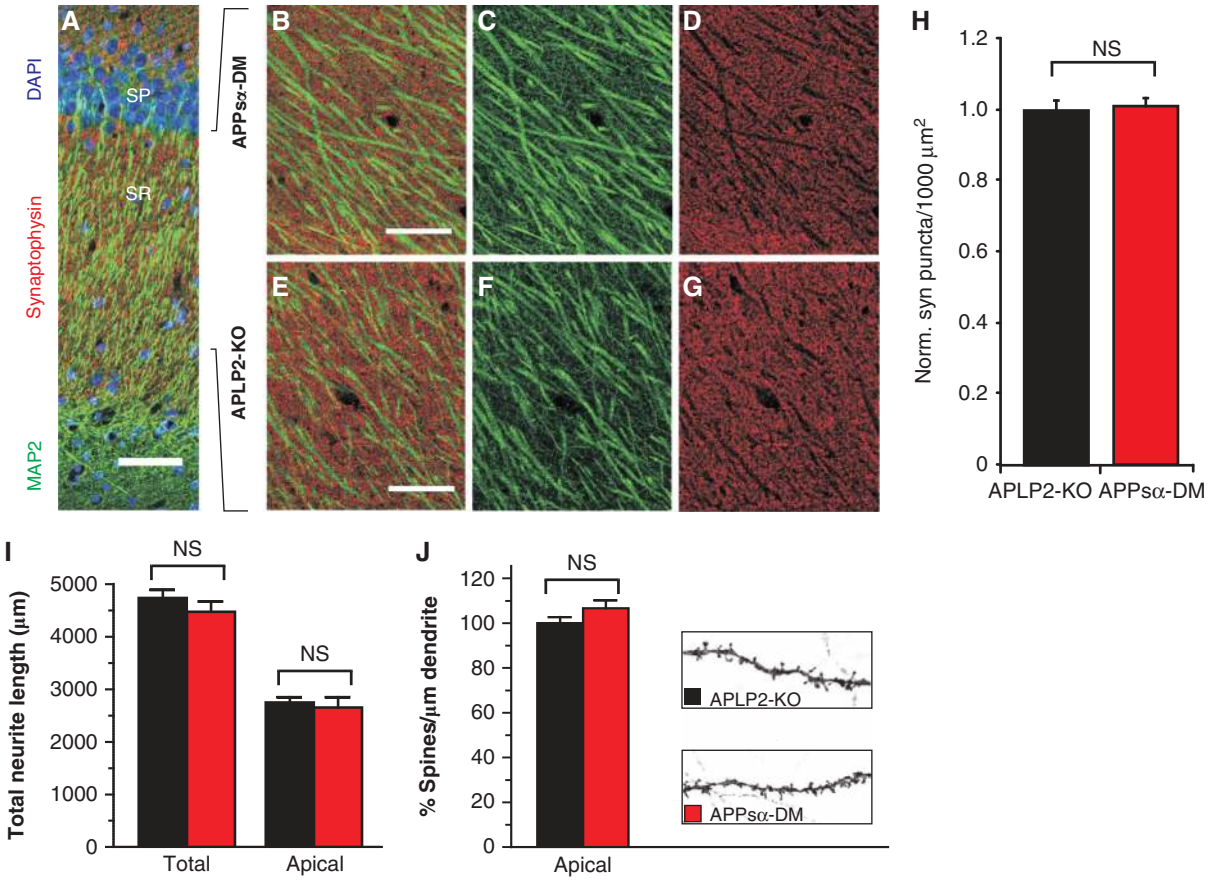

Figure 6 APPsα-DM mice show no alterations in synaptic density and neuronal morphology. (**A–G**) MAP2 and synaptophysin staining appeared similar in APPsα-DM mice (**B–D**) and APLP2 controls (**E–G**). (**H**) Quantification of synaptophysin-immunoreactive puncta in SR of hippocampal CA1 region. Puncta per 1000 µm^2 normalized to APLP2-KO. Data were obtained from 18 brain sections (3 mice/genotype, 3 sections/mouse) (ns, *t*-test). Scale bars: (**A**) = 50 µm, (**B**, **E**) = 25 µm; SR: striatum radiatum, SP: striatum pyramidale. (**I**, **J**) Morphology of CA1 pyramidal neurons in OTC. Neurite length was not significantly different (**I**). (**J**) Spine densities in mid-apical regions normalized to spine counts of APLP2-KO mice ($n = 36$ neurons/genotype, mean ± s.e.m.).

mice (Supplementary Figure S4 and data not shown). Transcellular adhesion of APP family proteins may promote synaptogenesis, as APP overexpression in HEK cells induced pre-synaptic specialization in co-cultured neurons (Wang *et al*, 2009). Since APPsα-DM mice lack cell surface APP/APLP2, we asked whether this may lead to impaired synaptogenesis and stained hippocampal sections for the dendritic marker MAP2 or the synaptic marker synaptophysin. APPsα-DM mice revealed a pattern that was indistinguishable from APLP2-KO control mice and quantification of synaptophysin-positive clusters failed to reveal significant differences (Figure 6A–H), excluding major alteration in synaptic density.

Several studies implicated APP in the control of neurite outgrowth and branching (Perez *et al*, 1997; Young-Pearse *et al*, 2008). We therefore analysed neuronal morphology in organotypic hippocampal cultures (OTCs). Quantitative analysis revealed unaltered neurite length (Figure 6I) and dendritic branching in APPsα-DM CA1 neurons (Supplementary Figure S4I–K). In addition, no significant alteration in spine density was detectable in the mid-distal portion of apical dendrites, corresponding roughly to the region in which CA3 axons terminate on CA1 dendrites (Figure 6J). Overall, these data suggest that lack of transmembrane APP/APLP2 isoforms does not affect dendritic structure and spine density of CA1 hippocampal pyramidal neurons.

APPsα-DM mice show strong deficits in hippocampus-dependent learning and memory

Because of their reduced muscle strength, spatial learning of APPsα-DM mice was not tested in the water-maze, but in dry mazes, a T-maze and on the 8-arm radial-maze. When given a free choice between the two arms during repeated exposures to a T-shaped maze with a delay of 30 s, normal mice show a strong tendency to choose the arm not visited during the previous trial. This spontaneous alternation was strongly reduced in APPsα-DM mice (Figure 7A; Supplementary Figure S8F).

When collecting eight baits from the eight freely accessible arms of the radial-maze, APPsα-DM mice entered arms from which they had already collected the bait more often than APLP2-KO controls and failed to improve during 10 days of training (Figure 7B). In both groups, the number of errors increased with the number of baits already collected, reflecting the increasing challenge of working memory, but in APPsα-DM this increase was significantly steeper than in APLP2-KO mice (Figure 7C). Taken together, the deficits in these two tasks are indicative of a spatial working memory deficit in APPsα-DM mice. APPsα-DM mice were also tested for two hippocampus-dependent species-typical behaviours, nesting behaviour, and burrowing behaviour. Both were massively impaired (Supplementary Figures S5 and S8G and H).

In order to assess learning in an environment that minimizes challenges on motor function and exposure to novelty, APPsα-DM mice were transferred to the IntelliCage (IC), a large home cage that permits automated behavioural testing of individual mice in a social context (see Supplementary Figure S6 for an overview of tests). In four learning corners, water can be accessed by making a nose poke. After an adaptation phase (Supplementary Figure S7), access to water was blocked by doors that could be opened with a nose poke, first at any time of the day, later only during two daily drinking sessions (11–12 h and 16–17 h). In order to test spatial learning, each mouse was assigned a single corner where it had to obtain its water. APPsα-DM mice were even more efficient than APLP2-KO controls at directing their visits to the rewarded corner (Figure 7D), demonstrating that they could master the sensory and motor demands of this type of task despite their muscular weakness and hyperactivity. To test reversal learning, availability of water was shifted to the opposite corner. APPsα-DM mice adapted more slowly (Figure 7D) because they persisted in visiting the previously correct corner (data not shown). The mice were then tested in a patrolling task in which access to water changes to the next clockwise corner after each rewarded visit. APPsα-DM mice were strongly impaired in learning this rule (Figure 7E). In summary, IC testing further corroborated defects in hippocampal function in APPsα-DM.

To gain further mechanistic insight into which domains/proteolytic fragments are crucial for hippocampal APP/APLP2-mediated functions, we first examined potential transcriptome changes, as AICD may regulate transcription in a Notch-like manner (Cao and Sudhof, 2001). However, microarray analysis of hippocampi and cortices from APPsα-DM and APLP2-KO controls failed to reveal any genotype-related transcriptional differences (Supplementary Figure S10; Supplementary Tables S1 and S2). Expression differences between cortex and hippocampus were, however, readily detectable (Supplementary Figure S10).

APPsα-DM mice exhibit impaired LTP, yet normal basal synaptic transmission and short-term plasticity

In APP-KO mice, LTP and behavioural deficits only develop in aged mice (Seabrook *et al*, 1999; Ring *et al*, 2007). In contrast, young adult APPsα-DM mice already showed deficits in T-maze performance. We therefore explored the possibility that LTP deficits in the CA3-CA1 Schaffer collateral pathway in hippocampal slices can be observed in young APPsα-DM mice. We induced LTP by an application of theta-burst stimulation (TBS) in either young adult (3–5 months old; Figure 8A)

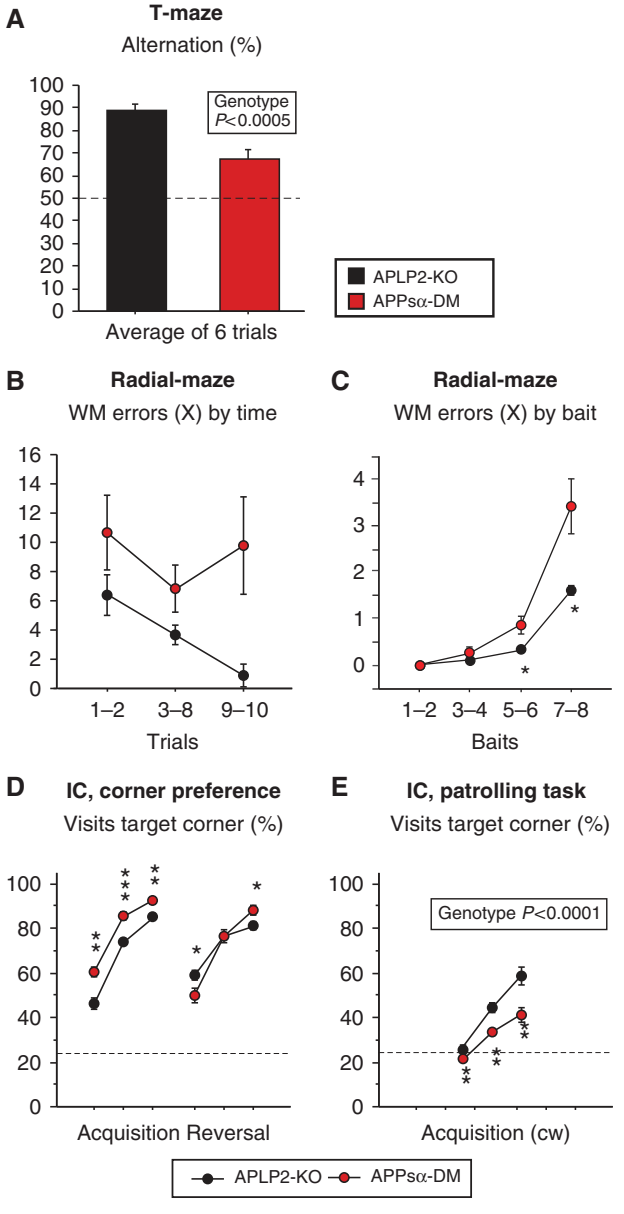

Figure 7 APPsα-DM mice show strong deficits in hippocampus-dependent learning and memory. (**A**) T-maze spontaneous alternation. % Alternations in six trials of task, chance level 50%. APPsα-DM mice showed less alternation than APLP2-KO mice (genotype $F(1,20)=17.4$ $P<0.0005$; one sample *t*-test versus 50%: APLP2-KO $t(13)=14.0$ $P<0.0001$, APPsα-DM $t(9)=3.9$ $P<0.0038$). APPsα-DM $n=10$, APLP2-KO $n=14$; graphs represent data pooled from two independent cohorts of female mice tested independently. (**B**) Radial-maze working memory (WM) errors by time. APLP2-KO control mice learned the test well, making less than two errors per trial at the end of training. APPsα-DM performed significantly worse, making on average 10 errors per trial at the beginning as well as at the end of training (genotype $F(1,7)=8.0$ $P<0.0256$, time $F(2,14)=3.4$ $P<0.0642$, time × genotype $F(2,14)=2.2$ ns; time split by genotype: APPsα-DM $F(2,6)=1.1$ ns, APLP2-KO $F(2,8)=6.9$ $P<0.0179$). APPsα-DM $n=4$, APLP2-KO $n=5$, all males. (**C**) Radial-maze, WM errors by bait. Working memory errors made before collection of baits 1–2, 3–4, 5–6, 7–8; averaged across trials. In both groups, the number of errors increased with the number of baits already collected, reflecting the increasing difficulty and challenge of working memory. In APPsα-DM, this increase was significantly steeper (genotype $F(1,7)=11.3$ $P<0.0121$, bait $F(3,21)=89.9$ $P<0.0001$, bait × genotype $F(3,21)=11.3$ $P<0.0001$). APPsα-DM $n=4$, APLP2-KO $n=5$, all males. (**D**) IC corner preference learning. Visits to the target corner during acquisition (sessions 1–2, 2–13, 13–14) and reversal (sessions 1–2, 3–7, 8–9), chance = 25% (dashed line). APPsα-DM preferred the target corner more strongly than APLP2-KO mice during acquisition were impaired at the beginning of reversal but were better at the end of the reversal (genotype $F(1,18)=7.0$ $P<0.0162$, phase × genotype $F(1,18)=31.7$ $P<0.0001$, time $F(2,36)=430.9$ $P<0.0001$, time × genotype $F(2,36)=2.5$ $P<0.0928$, time × phase × genotype $F(2,36)=12.5$ $P<0.0001$). APPsα-DM $n=9$, APLP2-KO $n=13$, all females. (**E**) IC patrolling task. Correct visits during sessions 1–2, 3–12, and 13–14. APPsα-DM showed strongly impaired learning (genotype $F(1,20)=13.9$ $P<0.0013$, time $F(2,40)=100.9$ $P<0.0001$, time × genotype $F(2,40)=5.6$ $P<0.0072$). APPsα-DM $n=9$, APLP2-KO $n=13$, all females. $^{***}P<0.001$, $^{**}P<0.01$, $^{*}P<0.05$.

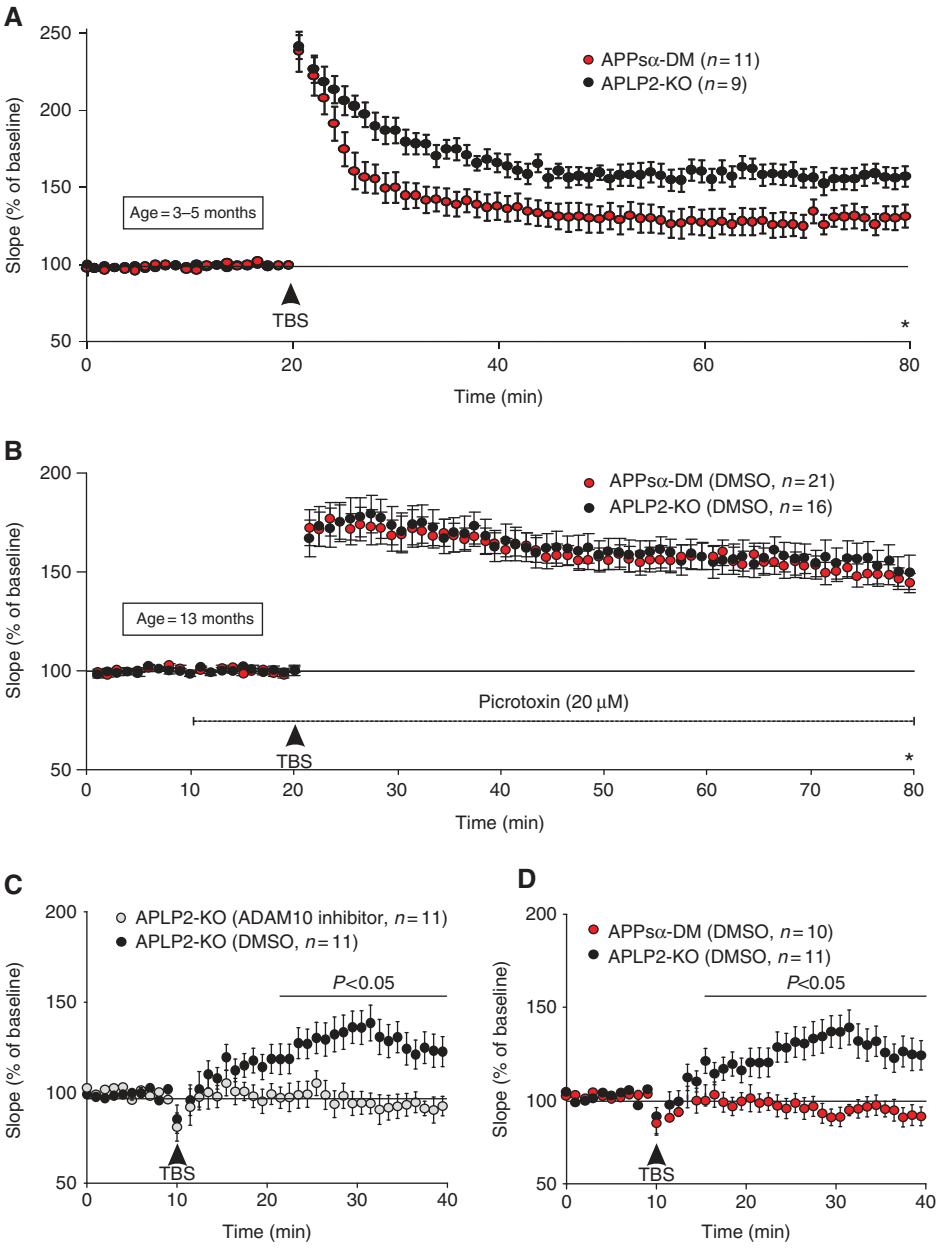

Figure 8 APPsα-DM mice exhibit impaired LTP. Schaffer collaterals of hippocampal slices of APPsα-DM mice or APLP2-KO mice were stimulated at 0.1 Hz (baseline) and fEPSPs recorded in CA1. Data points are averaged over six time points, mean baseline slope was set to 100%. (**A**) LTP of fEPSP was induced by application of TBS after 20 min baseline stimulation (arrowhead). Sixty minutes after TBS (asterisk) a significant difference between acute slices of APPsα-DM and APLP2-KO mice could be observed ($P=0.001$, *t*-test); $n=$number of slices. (**B**) In acute slices from APPsα-DM or APLP2-KO mice picrotoxin (20 μM) was added 10 min after starting baseline recording and a TBS was applied 10 min later. The average potentiation was statistically indistinguishable between APPsα-DM ($151.9\pm8.7\%$, $n=16$) or APLP2-KO ($147.1\pm9.8\%$, $n=21$; $P=0.44$, *t*-test). (**C**) In organotypic hippocampal cultures LTP of fEPSP was induced by TBS after 10 min of baseline recording (arrowhead). Ten to thirty minutes after TBS a significant difference between APLP2-KO (control with 0.01% DMSO, black circles) and APLP2-KO cultures treated with ADAM10 inhibitor (grey circles) could be observed ($P=0.036$, *t*-test). (**D**) APLP2-KO and APPsα-DM organotypic cultures were compared, both in 0.01% DMSO. Note that APPsα-DM cultures lacked potentiation and were statistically indistinguishable from inhibitor-treated APLP2-KO cultures plotted in panel (**C**) ($P=0.65$).

or aged (10–13 months; Supplementary Figure S11A) APPsα-DM, APLP2-KO or WT mice after baseline recording. At both ages, APPsα-DM slices showed already a lower LTP during the induction phase, which resulted in a significant difference 55–60 min after TBS compared with APLP2-KO littermate controls or WT slices. The average potentiation in APPsα-DM slices (3–5 months old; Figure 8A) was $129\pm5.1\%$ ($n=10$), whereas APLP2-KO slices showed a potentiation of $158\pm6.2\%$, ($n=8$), 55–60 min after the TBS ($P=0.014$, *t*-test). Highly similar results were obtained in aged mice (Supplementary Figure S11A). APLP2-KO mice showed no LTP phenotype different from WT at any age tested.

To investigate whether the defect in LTP in APPsα-DM mice is due to changes in pre-synaptic components necessary to support LTP, we examined short-term plasticity by measuring PPF. However, no significant differences at any interstimulus

interval tested (Supplementary Figure S11B), nor differences in basal synaptic properties (as assessed by input–output curves; Supplementary Figure S11C) were detectable. Thus, in contrast to peripheral synapses of the NMJ, pre-synaptic defects in transmitter release were absent in glutamatergic hippocampal CA3/CA1 synapses. APP-KO mice have an increased susceptibility to kainite-induced seizures (Steinbach *et al*, 1998) and their LTP deficit could be rescued by inhibition of $GABA_A$ receptors (Fitzjohn *et al*, 2000). Therefore, we tested for a potential inhibitory GABAergic contribution to the potentiation defect in APPsα-DM mice. In acute slices picrotoxin (20 μM) was added 10 min after baseline recording and a TBS was applied 10 min later (Figure 8B). The average potentiation was now statistically indistinguishable between APPsα-DM slices (151.9 ± 8.7%, $n = 16$) or APLP2-KO controls (147.1 ± 9.8%, $n = 21$; $P = 0.44$, *t*-test). Thus, $GABA_A$-R-mediated inhibition is likely altered in APPsα-DM mice and may thus contribute to reduced ability to induce and maintain LTP.

Functional role of APP/APLP2 domains

Next, we studied more closely the specific role of APPsα for LTP and asked whether inhibition of α-secretase-mediated release of APPsα in APLP2-KO mice (or APLP2sα release in APP-KO mice) would affect LTP. As short-term α-secretase inhibition had no effect on LTP in acute slices, we switched to OTCs that were treated with the ADAM10 inhibitor GI254023X for 5 days. Indeed, inhibitor treatment of APLP2-KO OTCs resulted in a significant reduction in LTP (Figure 8C). The average potentiation in APLP2-KO cultures (control, treated with 0.01% DMSO) was 123.4 ± 6.2% ($n = 11$), whereas cultures treated with the ADAM10 inhibitor showed no LTP (93.3 ± 5.1%; $n = 11$; $P = 0.034$, *t*-test; 35–40 min after TBS). This implies that a transient increase in APPsα or another ADAM10 substrate is required for LTP. Due to less cooperativity in thin OTCs the overall potentiation was lower than in acute slices. To our surprise, when recording from APPsα-DM cultures, which readily express APPsα (and APLP1 as another ADAM10 substrate), we were unable to detect any residual LTP even without inhibitor treatment (Figure 8D: average potentiation of 90.2 ± 4.1%; $n = 10$; $P = 0.031$; 35–40 min after TBS). Responses were statistically indistinguishable from ADAM10 inhibitor-treated APLP2-KO cultures ($P = 0.65$). No additional effect on APPsα-DM cultures was detectable upon inhibitor treatment (data not shown). Surprisingly, the blockade of α-secretase-mediated APPsα release in APLP2-KO mice has the same effect as the genetic modification in APPsα-DM mice, for which all APP is soluble APPsα. Thus, although APPsα-DM mice still produce APPsα, this constitutive APPsα secretion may not be sufficient for normal LTP responses (see Discussion). Interestingly, ADAM10 inhibition in APP-KO organotypic slices also showed lower LTP induction rates. On average, APP-KO cultures showed a potentiation of 120.7 ± 8.1%, $n = 8$, whereas inhibitor-treated APP-KO cultures showed almost no potentiation (Supplementary Figure S11D; 102.3 ± 7.9%; $n = 9$; $P = 0.02$, two-way ANOVA (11–40 min, including all post-TBS values; or $P = 0.069$, assessed by *t*-test; 35–40 min after TBS), suggesting that APLP2sα release may contribute to normal LTP responses.

Discussion

Here, we report on several novel synaptic functions of APP family proteins in both PNS and CNS. The first key finding is that expression of the secreted ectodomain APPsα is sufficient to circumvent the postnatal lethality of the majority of APP/APLP2-DKO mice. Surviving APPsα-DM mice are, however, not normal but represent a very informative hypomorph with an intermediate phenotype as compared with lethal DKO mice or viable single KOs and wild-type mice (see Supplementary Table S3 for summary). Phenotypic aspects of APPsα-DM mice that are ameliorated compared with DKO mice (lacking holo-APP, APLP2 and all proteolytic fragments derived from them) indicate a functional rescue due to APPsα expression. Conversely, abnormalities in APPsα-DM mice not observed in either APLP2-KO or APP-KO mice (lacking holo-APP, APPsα, APPsβ, Aβ, CTFs, and AICD), are likely due to a lack of redundant functions mediated synergistically by APP and APLP2 that had been masked in single mutants and could not be assessed in double mutants due to perinatal death.

NMJ phenotype

Here, we show that APLP2 and specific domains of APP are essential for several key steps in NMJ development. As both APPsα-DM and DKO mice (Supplementary Table S3) exhibit widened endplate bands and excessive nerve growth, it appears that APPsα expression is not sufficient to compensate for these early developmental defects. In contrast, impairments of neurotransmission in adult APPsα-DM mice (highly variable frequency of spontaneous MEPPs, a reduction in quantal content of evoked responses, a smaller RRP of vesicles) were much milder than those of perinatal lethal DKO mice (with over 50% of fibres completely lacking MEPPs and 25% of fibres lacking evoked responses; Wang *et al*, 2005). Thus, APPsα ameliorates the pre-synaptic defect in transmitter release of DKO mice to a level sufficient for survival of the majority of animals. We hypothesize that a more severe defect in neurotransmission underlies the loss of about 40% of APPsα-DM animals at around birth. Our findings contrast with the failure of APPsβ-KI mice to rescue the lethality of APP/APLP2-DKO mice (Li *et al*, 2010) and suggest distinct physiological functions of secreted APP ectodomains. Consistent with our results, APPsβ has previously been found far less potent in neuroprotection (Furukawa *et al*, 1996; Copanaki *et al*, 2010), and has recently even been linked with degenerative processes (Nikolaev *et al*, 2009).

APP and APLP2 are cell surface proteins expressed by motoneurons, as well as post-synaptic muscle cells. Although our data do not rule out an adhesive function of APP/APLPs during initial stages of NMJ synaptogenesis, they challenge the concept that lack of APP/APLP mediated trans-synaptic adhesion is the primary cause of synaptic dysfunction and perinatal lethality of DKO mice (Wang *et al*, 2009). Instead our findings highlight the importance of APPsα as a secreted signalling factor required for synaptic function. Interestingly, upon differentiation of aneural cultures of C2C12 myoblasts large amounts of APPsα are secreted (Supplementary Figure S1E). It is well established that secreted molecules (e.g., FGF, GDNF and ECM components) can regulate pre-synaptic differentiation including transmitter release (reviewed in Wu *et al* (2010)). As APPsα has previously been shown to modulate ion channel activity

(including NMDA receptors; Furukawa and Mattson, 1998; Taylor *et al*, 2008), it is tempting to speculate that APPsα may modulate transmitter release, via binding to an as yet unknown pre-synaptic cell surface receptor. Alternatively, APPsα may function by interacting with basal lamina components within the synaptic cleft.

The impaired transmitter release in APPsα-DM mice is consistent with their severe muscular weakness in demanding neuromotor tasks. The NMJ normally has a large safety factor since EPP depolarization is typically 2–5-fold greater than threshold for generation of a muscle action potential (Wood and Slater, 1997). Thus, the 45% reduction in quantal content for a single stimulus in APPsα-DM muscles (Figure 2D) is not expected to compromise synaptic transmission for basal locomotion (Hennig and Lomo, 1985). When a large force needs to be maintained, however, the combination of (1) low initial quantal content, (2) small RRP, and (3) reduced replenishment of the RRP is likely to produce failure of synaptic transmission and muscle weakness (Figure 1A–C).

Our finding of severely reduced RRP is consistent with EM studies showing smaller active zones containing fewer docked vesicles in newborn APP/APLP2-DKO animals (Yang *et al*, 2005). The smaller pre-synaptic area (Figure 5C) of APPsα-DM is, however, not enough to account for the reduced quantal content or RRP. In addition, APPsα-DM NMJ synapses show an impaired ability to maintain sustained vesicle release, suggesting a more direct role of APP/APLP2 for exocytosis. What pre-synaptic molecules might interact with the cytoplasmic domains of APP and APLP2 to mediate this effect? Among known APP interactors Mint2 (and to a lesser extent Mint1) is highly expressed in rodent spinal cord (Ho *et al*, 2003) and motoneurons (Yao *et al*, 2011) and the single drosophila homologue dX11 has been implicated in the formation of new synapses at the drosophila NMJ (Ashley *et al*, 2005). Here, we show by immunoprecipitation and BiFC analysis in living cells that binding of Mint2 to the APP C-terminus can recruit Munc18-1 into a tripartite complex, which may thus link APP to the NMJ exocytic machinery (reviewed by Rizo and Rosenmund (2008) and Neher and Sakaba (2008)). Overall, our data suggest that lack of APP/APLP2 transmembrane isoforms in APPsα-DM mice abolishes APP/Mint2/Munc18 complex formation and may thus perturb the organization and/or regulation of the NMJ exocytic complex. Future experiments will be required to demonstrate that the tripartite complex is required for normal replenishment of vesicles for exocytosis.

Another novel finding of our study is that APP and APLP2 are essential for postnatal maturation and maintenance of neuromuscular synapses. This was evident from the significant increase in fragmented endplates and persistence of immature plaque-like post-synaptic specializations in adult APPsα-DM. Notably, this phenotype emerged in young adult animals (aged 8 weeks) whereas juvenile APPsα-DM were not affected. Similar phenotypes were observed in mice deficient for muscle proteins or ECM components (e.g., Gonzalez *et al*, 1999; Kong and Anderson, 1999; Fox *et al*, 2007, 2008). Collectively, our data identify APP and APLP2 as key molecules required (1) during early stages of nerve growth and synaptic pattern formation, (2) from around birth onwards to mediate efficient and sustained transmitter release, and (3) postnatally for the maturation and/or maintenance of the post-synaptic apparatus.

CNS phenotype

The viability of APPsα-DM mice made it possible for the first time to study the physiological role of APP and APLP2 for the adult central nervous system. In contrast to the morphological defects observed for peripheral neuromuscular synapses, APPsα-DM mice showed no gross alterations in cortical or hippocampal architecture and no detectable difference in neurite and synaptic cluster density. Moreover, APPsα-DM mice showed unaltered morphology of pyramidal neurons without significant alterations in neurite length, dendritic branching, or spine density in apical aspects of hippocampal CA1 dendrites. We therefore conclude that, at least with regard to the morphological aspects tested here, cell surface APP/APLP2 isoforms are not essential, and hippocampal synapse formation proceeds normally in the absence of APP/APLP2-mediated adhesion. Although we could not detect any upregulation of APLP1 (Supplementary Figure S1D), we cannot formally exclude APLP1-mediated compensatory effects.

Consistent with this, APPsα-DM mice showed normal basal synaptic transmission between CA3/CA1 pyramidal cells, unaltered short-term plasticity and thus, no alterations in pre-synaptic transmitter release. Despite this, we observed severe hippocampus-dependent behavioural deficits that were associated with a pronounced impairment in the induction and maintenance of LTP, already in young adult APPsα-DM mice. The comparison of young APLP2-KO with wild-type animals showed that APLP2 deficiency on its own does not result in LTP defects (Supplementary Figure S11A). To delineate the underlying mechanisms of the LTP deficit, we could exclude impaired AICD-mediated transcriptional responses. We next considered mechanisms depending on membrane attachment such as adhesion and/or trans-cellular signalling mediated by APP homo-dimers or via binding to other cell surface molecules. Strikingly, treatment of APLP2-KO OTCs with an ADAM10 inhibitor completely impaired LTP. Thus, given that inhibition of APP ectodomain shedding will increase APP cell surface isoforms, our finding that α-secretase inhibition leads to impaired LTP argues against a major role of transmembrane APP signalling for LTP induction and maintenance. Another possibility that we cannot rule out is that the effect of the ADAM10 inhibitor is mediated by inhibition of substrates other than APP. Previously, we showed that APPsα is produced and secreted in APPsα-KI brains at high levels and is readily detectable in supernatants of mouse embryo fibroblasts (Ring *et al*, 2007). However, the finding that APPsα expression from the KI allele leads to the same LTP deficit as ADAM10 inhibition in APLP2-KO slices (see Figure 8C and D) suggests that unregulated/constitutive APPsα expression may lead to insufficient local amounts or abnormal timing of APPsα release at the synapses during LTP induction. We are also aware that infusion of high amounts of recAPPsα into rat brain may inhibit LTP (Taylor *et al*, 2008). However, as APPsα-KI single mutants displayed a wild-type-like phenotype without LTP impairment (Ring *et al*, 2007), we consider insufficient APPsα production in APPsα-DM mice more likely than a transdominant inhibitory effect.

Our data are consistent with a model (Figure 9) in which regulated cleavage of APP to form endogenous APPsα during synaptic activity is required to enhance NMDA-R signalling during LTP. Indeed, APPsα secretion has been shown to be enhanced by neuronal depolarization (Gakhar-Koppole *et al*,

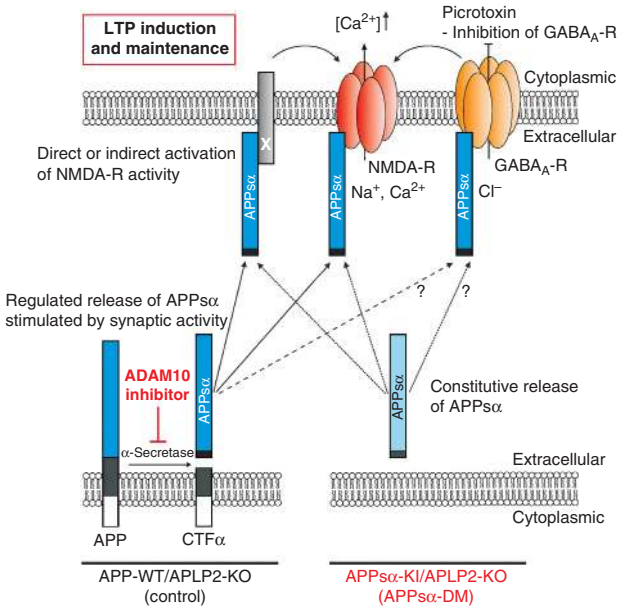

Figure 9 Role of APPsα in LTP facilitation. Left: regulated release of APPsα during synaptic activity may directly or indirectly enhance NMDA-R signalling needed for LTP induction and maintenance. Alternatively, APPsα may also reduce $GABA_A$-R-mediated inhibition. Inhibition of α-secretase by GI254023X abolishes APPsα release and thus LTP in APLP2-KO mice. Right: constitutive release of APPsα in APPsα-DM mice may be too low for normal LTP responses.

2008), high frequency stimulation (Mills and Reiner, 1999; Fazeli *et al*, 1994), and by activation of metabotropic glutamate receptor, or muscarinic AChRs (Nitsch *et al*, 1992, 1998). Consistent with our data, Taylor *et al* (2008) showed that hippocampal infusion of APPsα-specific antibodies or α-secretase inhibitors not only impaired LTP but also reduced tetanically evoked NMDA receptor currents. APPsα signalling involving NMDA receptor activation is also well in agreement with our finding that $GABA_A$-R inhibition, that facilitates post-synaptic depolarization (Figure 9), rescued the LTP deficit of APPsα-DM mice. Alternatively, it cannot be excluded that APPsα might also directly regulate GABAergic inhibition (Figure 9). Although neuromuscular synapses and hippocampal CA3/CA1 synapses are both excitatory, they also exhibit clear differences, e.g., regarding the number/structure of release sites and quantal content, with a much higher demand on transmitter release at the NMJ (Neher and Sakaba, 2008). Thus, while pre-synaptic release at glutamatergic CA3/CA1 synapses is unaffected in APPsα-DM mice, network properties of hippocampal circuits might be compromised by lack of APP/APLP2, as suggested by the increased kainite susceptibility of APP-KO mice (Steinbach *et al*, 1998).

Previously, we showed that on an APLP2 wild-type background APPsα-KI mice are phenotypically normal (Ring *et al*, 2007). Given that learning and LTP deficits in APP-KO mice emerged only upon aging (suggesting compensation by APLP2) and that constitutive APPsα release may become insufficient in the absence of APLP2, our findings indicate that APLP2 (likely via secretion of APLP2sα; Eggert *et al*, 2004; Endres *et al*, 2005; see Supplementary Figure S11D) is synergistically required in addition to APP for LTP, learning, and memory. Here, we show that APPsα-DM mice exhibited a defect in spatial working memory, as evidenced by impairments in T-maze alternation (Deacon and Rawlins, 2006) and in the radial-maze (Olton *et al*, 1978; Rossi-Arnaud *et al*, 1991). Also, the deficit in the patrolling task of IC can be interpreted along these lines because the mice must remember in which corner they last obtained reward in order to learn the correct response pattern. In addition, APPsα-DM mice displayed behavioural changes typical for rodents with hippocampal dysfunction, notably the impairments in the nesting and burrowing test (Deacon *et al*, 2002), impaired exploration and habituation in the open field and IC (Roberts *et al*, 1962; Colacicco *et al*, 2009), and perseverative behaviour (Hirsh, 1970). This requirement of APP and APLP2 for normal CNS function contrasts with the normal differentiation and electrophysiological properties of cultured neurons lacking all three APP family members (Bergmans *et al*, 2010) and highlights the importance to study APP family functions in the living organism.

Collectively, our study identifies APP and APLP2 as essential for both peripheral and central nervous system functions. As reduced levels of APPsα have been suggested to contribute to the cognitive impairment and pathogenesis of AD, our data warrant the study of potential alterations of APLP2 expression and processing during AD pathogenesis and aging. Our data also imply that care must be taken when developing pharmacotherapy for AD to avoid compromising endogenous APP/APLP2 functions.

Materials and methods

Mice

APPsα-KI and APLP2-KO were mated to obtain $APP^{s\alpha/wt}/APLP2^{-/-}$ mice that were further intercrossed to obtain APPsα-DM ($APP^{s\alpha/s\alpha}/APLP2^{-/-}$) and the corresponding APLP2-KO littermate controls (see Supplementary data).

Western blot analysis and CNS immunostaining

See Supplementary data.

NMJ immunohistochemistry

Diaphragms were dissected, incubated in 1 mg/ml type-IA collagenase (Sigma) in PBS supplemented with 0.036 mM $CaCl_2$ for 15 min at room temperature (RT), rinsed in PBS, and fixed in 1% formaldehyde/PBS for 1 h at RT. Tissue was permeabilized (1% Triton X-100/PBS) and incubated with the following antibodies: neurofilament (1:500, rabbit polyclonal, Chemicon) or against synaptophysin (1:50, rabbit polyclonal, Invitrogen) in 2% BSA/PBS at 4°C for 48 h followed by staining with MFP-488 conjugated goat α-rabbit antibody (1:100, Molecular Biotechnology) and rhodamine-conjugated α-bungarotoxin (1:500; Invitrogen) in 2% BSA/PBS at 4°C and mounted in Mowiol 4-88 (Carl Roth). Images were obtained with a Nikon A1R CLSM. For details see Supplementary data.

Electrophysiology

The diaphragm with 5–10 mm of the attached phrenic nerve was dissected from adult mice (7–8 weeks old), mounted in a Sylgard-lined dish, and superfused with oxygenated (95% O_2/5% CO_2) modified Tyrode's solution (in mM: 125 NaCl, 5.37 KCl, 24 $NaHCO_3$, 1 $MgCl_2$, 1.8 $CaCl_2$, 11 glucose, pH 7.4) for at least 1 h before recording. Hippocampal slices were prepared from APPsα-DM, APLP2-KO mice, or wild-type mice according to standard procedures. Electrophysiological recordings were performed as previously described (Ring *et al*, 2007) and detailed in Supplementary data.

Behaviour

All behavioural procedures were approved by animal welfare authorities. A total of 31 mice (six times backcrossed to C57BL/6,

APPsα-DM $n = 13$: 10 female, 3 male; APLP2-KO controls: $n = 18$, 14 female, 4 male), distributed over two cohorts (cohort 1: all female; cohort 2: males and females), were analysed in a blinded manner. For several parameters females of cohorts 1 and 2 were pooled. In addition, we also analysed animals of both sexes (cohort 2) to show that behavioural alterations are independent of sex (Supplementary Figure S9). For details see Supplementary data.

Supplementary data
Supplementary data are available at *The EMBO Journal* Online (http://www.embojournal.org).

Acknowledgements

We thank V Witzemann, F Chevessier, and V von Bohlen for advice with diaphragm histology, T Deller for advice regarding GI254023X treatment, P Mathews for providing anti-APPsα antibodies, the Nikon Imaging Centre (Heidelberg), and J Gobbert, I Drescher and M Neumann for excellent technical assistance; M Zagrebelsky and Diane Mundil for preparing organotypic cultures for electrophysiological analysis. We thank N Gretz for performing Microarray hybridizations. This work was supported by grants from DFG (SFB 488/D18, MK1457/8-1 to UM), BMBF (01GS08128 to UM), the Thyssen Foundation (to UM and MK), the Breuer Stiftung (to UM), Univ. of Colorado SIRC (to JC), Swiss NF and NCCR Neural Plasticity and Repair (to DPW).

Conflict of interest

The authors declare that they have no conflict of interest.

References

Anliker B, Müller U (2006) The functions of mammalian amyloid precursor protein and related amyloid precursor-like proteins. *Neurodegener Dis* **3:** 239–246

Ashley J, Packard M, Ataman B, Budnik V (2005) Fasciclin II signals new synapse formation through amyloid precursor protein and the scaffolding protein dX11/Mint. *J Neurosci* **25:** 5943–5955

Bergmans BA, Shariati SA, Habets RL, Verstreken P, Schoonjans L, Müller U, Dotti CG, De Strooper B (2010) Neurons generated from APP/APLP1/APLP2 triple knockout embryonic stem cells behave normally *in vitro* and *in vivo*: lack of evidence for a cell autonomous role of the amyloid precursor protein in neuronal differentiation. *Stem Cells* **28:** 399–406

Cao X, Sudhof TC (2001) A transcriptionally [correction of transcriptively] active complex of APP with Fe65 and histone acetyltransferase Tip60. *Science* **293:** 115–120

Colacicco G, Voikar V, Vannoni E, Lipp H-P, Wolfer DP (2009) Cognitive functions of hippocampus lesioned mice assessed in the IntelliCage. *Neuroscience Meeting Planner Society for Neuroscience*, 2009 Program No 47819 2009

Copanaki E, Chang S, Vlachos A, Tschape JA, Muller UC, Kogel D, Deller T (2010) sAPPalpha antagonizes dendritic degeneration and neuron death triggered by proteasomal stress. *Mol Cell Neurosci* **44:** 386–393

Deacon RM, Croucher A, Rawlins JN (2002) Hippocampal cytotoxic lesion effects on species-typical behaviours in mice. *Behav Brain Res* **132:** 203–213

Deacon RM, Rawlins JN (2006) T-maze alternation in the rodent. *Nat Protoc* **1:** 7–12

Eggert S, Paliga K, Soba P, Evin G, Masters CL, Weidemann A, Beyreuther K (2004) The proteolytic processing of the amyloid precursor protein gene family members APLP-1 and APLP-2 involves alpha-, beta-, gamma-, and epsilon-like cleavages: modulation of APLP-1 processing by n-glycosylation. *J Biol Chem* **279:** 18146–18156

Elmqvist D, Quastel DM (1965) A quantitative study of end-plate potentials in isolated human muscle. *J Physiol* **178:** 505–529

Endres K, Postina R, Schroeder A, Mueller U, Fahrenholz F (2005) Shedding of the amyloid precursor protein-like protein APLP2 by disintegrin-metalloproteinases. *FEBS J* **272:** 5808–5820

Fazeli MS, Breen K, Errington ML, Bliss TV (1994) Increase in extracellular NCAM and amyloid precursor protein following induction of long-term potentiation in the dentate gyrus of anaesthetized rats. *Neurosci Lett* **169:** 77–80

Fitzjohn SM, Morton RA, Kuenzi F, Davies CH, Seabrook GR, Collingridge GL (2000) Similar levels of long-term potentiation in amyloid precursor protein -null and wild-type mice in the CA1 region of picrotoxin treated slices. *Neurosci Lett* **288:** 9–12

Fox MA, Ho MS, Smyth N, Sanes JR (2008) A synaptic nidogen: developmental regulation and role of nidogen-2 at the neuromuscular junction. *Neural Dev* **3:** 24

Fox MA, Sanes JR, Borza DB, Eswarakumar VP, Fassler R, Hudson BG, John SW, Ninomiya Y, Pedchenko V, Pfaff SL, Rheault MN, Sado Y, Segal Y, Werle MJ, Umemori H (2007) Distinct target-derived signals organize formation, maturation, and maintenance of motor nerve terminals. *Cell* **129:** 179–193

Furukawa K, Mattson MP (1998) Secreted amyloid precursor protein alpha selectively suppresses N-methyl-D-aspartate currents in hippocampal neurons: involvement of cyclic GMP. *Neuroscience* **83:** 429–438

Furukawa K, Sopher BL, Rydel RE, Begley JG, Pham DG, Martin GM, Fox M, Mattson MP (1996) Increased activity-regulating and neuroprotective efficacy of alpha-secretase-derived secreted amyloid precursor protein conferred by a C-terminal heparin-binding domain. *J Neurochem* **67:** 1882–1896

Gakhar-Koppole N, Hundeshagen P, Mandl C, Weyer SW, Allinquant B, Muller U, Ciccolini F (2008) Activity requires soluble amyloid precursor protein alpha to promote neurite outgrowth in neural stem cell-derived neurons via activation of the MAPK pathway. *Eur J Neurosci* **28:** 871–882

Gonzalez M, Ruggiero FP, Chang Q, Shi YJ, Rich MM, Kraner S, Balice-Gordon RJ (1999) Disruption of Trkb-mediated signaling induces disassembly of postsynaptic receptor clusters at neuromuscular junctions. *Neuron* **24:** 567–583

Heber S, Herms J, Gajic V, Hainfellner J, Aguzzi A, Rulicke T, von Kretzschmar H, von Koch C, Sisodia S, Tremml P, Lipp HP, Wolfer DP, Müller U (2000) Mice with combined gene knock-outs reveal essential and partially redundant functions of amyloid precursor protein family members. *J Neurosci* **20:** 7951–7963

Hennig R, Lomo T (1985) Firing patterns of motor units in normal rats. *Nature* **314:** 164–166

Herms J, Anliker B, Heber S, Ring S, Fuhrmann M, Kretzschmar H, Sisodia S, Müller U (2004) Cortical dysplasia resembling human type 2 lissencephaly in mice lacking all three APP family members. *EMBO J* **23:** 4106–4115

Hirsh R (1970) Lack of variability or perseveration: describing the effect of hippocampal ablation. *Physiol Behav* **5:** 1249–1254

Ho A, Morishita W, Hammer RE, Malenka RC, Sudhof TC (2003) A role for Mints in transmitter release: Mint 1 knockout mice exhibit impaired GABAergic synaptic transmission. *Proc Natl Acad Sci USA* **100:** 1409–1414

Hornsten A, Lieberthal J, Fadia S, Malins R, Ha L, Xu X, Daigle I, Markowitz M, O'Connor G, Plasterk R, Li C (2007) APL-1, a Caenorhabditis elegans protein related to the human beta-amyloid precursor protein, is essential for viability. *Proc Natl Acad Sci USA* **104:** 1971–1976

Kerppola TK (2008) Bimolecular fluorescence complementation (BiFC) analysis as a probe of protein interactions in living cells. *Annu Rev Biophys* **37:** 465–487

Kong J, Anderson JE (1999) Dystrophin is required for organizing large acetylcholine receptor aggregates. *Brain Res* **839:** 298–304

Lannfelt L, Basun H, Wahlund LO, Rowe BA, Wagner SL (1995) Decreased alpha-secretase-cleaved amyloid precursor protein as a diagnostic marker for Alzheimer's disease. *Nat Med* **1:** 829–832

Li H, Wang B, Wang Z, Guo Q, Tabuchi K, Hammer RE, Sudhof TC, Zheng H (2010) Soluble amyloid precursor protein (APP) regulates transthyretin and Klotho gene expression without rescuing the essential function of APP. *Proc Natl Acad Sci USA* **107:** 17362–17367

Mills J, Reiner PB (1999) Mitogen-activated protein kinase is involved in N-methyl-D-aspartate receptor regulation of amyloid precursor protein cleavage. *Neuroscience* **94:** 1333–1338

Nikolaev A, McLaughlin T, O'Leary DD, Tessier-Lavigne M (2009) APP binds DR6 to trigger axon pruning and neuron death via distinct caspases. *Nature* **457:** 981–989

Neher E, Sakaba T (2008) Multiple roles of calcium ions in the regulation of neurotransmitter release. *Neuron* **59:** 861–872

Nitsch RM, Rossner S, Albrecht C, Mayhaus M, Enderich J, Schliebs R, Wegner M, Arendt T, von der Kammer H (1998) Muscarinic acetylcholine receptors activate the acetylcholinesterase gene promoter. *J Physiol Paris* **92:** 257–264

Nitsch RM, Slack BE, Wurtman RJ, Growdon JH (1992) Release of Alzheimer amyloid precursor derivatives stimulated by activation of muscarinic acetylcholine receptors. *Science* **258:** 304–307

Olton DS, Walker JA, Gage FH (1978) Hippocampal connections and spatial discrimination. *Brain Res* **139:** 295–308

Perez RG, Zheng H, Van der Ploeg LH, Koo EH (1997) The beta-amyloid precursor protein of Alzheimer's disease enhances neuron viability and modulates neuronal polarity. *J Neurosci* **17:** 9407–9414

Ring S, Weyer SW, Kilian SB, Waldron E, Pietrzik CU, Filippov MA, Herms J, Buchholz C, Eckman CB, Korte M, Wolfer DP, Müller UC (2007) The secreted beta-amyloid precursor protein ectodomain APPs alpha is sufficient to rescue the anatomical, behavioral, and electrophysiological abnormalities of APP-deficient mice. *J Neurosci* **27:** 7817–7826

Rizo J, Rosenmund C (2008) Synaptic vesicle fusion. *Nat Struct Mol Biol* **15:** 665–674

Roberts WW, Dember WN, Brodwick M (1962) Alternation and exploration in rats with hippocampal lesions. *J Comp Physiol Psychol* **55:** 695–700

Rogelj B, Mitchell JC, Miller CC, McLoughlin DM (2006) The X11/Mint family of adaptor proteins. *Brain Res Rev* **52:** 305–315

Rossi-Arnaud C, Fagioli S, Ammassari-Teule M (1991) Spatial learning in two inbred strains of mice: genotype-dependent effect of amygdaloid and hippocampal lesions. *Behav Brain Res* **45:** 9–16

Sanes JR, Lichtman JW (1999) Development of the vertebrate neuromuscular junction. *Annu Rev Neurosci* **22:** 389–442

Seabrook GR, Smith DW, Bowery BJ, Easter A, Reynolds T, Fitzjohn SM, Morton RA, Zheng H, Dawson GR, Sirinathsinghji DJ, Davies CH, Collingridge GL, Hill RG (1999) Mechanisms contributing to the deficits in hippocampal synaptic plasticity in mice lacking amyloid precursor protein. *Neuropharmacology* **38:** 349–359

Steinbach JP, Muller U, Leist M, Li ZW, Nicotera P, Aguzzi A (1998) Hypersensitivity to seizures in beta-amyloid precursor protein deficient mice. *Cell Death Differ* **5:** 858–866

Szodorai A, Kuan YH, Hunzelmann S, Engel U, Sakane A, Sasaki T, Takai Y, Kirsch J, Müller U, Beyreuther K, Brady S, Morfini G, Kins S (2009) APP anterograde transport requires Rab3A GTPase activity for assembly of the transport vesicle. *J Neurosci* **29:** 14534–14544

Taylor CJ, Ireland DR, Ballagh I, Bourne K, Marechal NM, Turner PR, Bilkey DK, Tate WP, Abraham WC (2008) Endogenous secreted amyloid precursor protein-alpha regulates hippocampal NMDA receptor function, long-term potentiation and spatial memory. *Neurobiol Dis* **31:** 250–260

Walsh DM, Minogue AM, Sala Frigerio C, Fadeeva JV, Wasco W, Selkoe DJ (2007) The APP family of proteins: similarities and differences. *Biochem Soc Trans* **35:** 416–420

Wang P, Yang G, Mosier DR, Chang P, Zaidi T, Gong YD, Zhao NM, Dominguez B, Lee KF, Gan WB, Zheng H (2005) Defective neuromuscular synapses in mice lacking amyloid precursor protein (APP) and APP-Like protein 2. *J Neurosci* **25:** 1219–1225

Wang Z, Wang B, Yang L, Guo Q, Aithmitti N, Songyang Z, Zheng H (2009) Presynaptic and postsynaptic interaction of the amyloid precursor protein promotes peripheral and central synaptogenesis. *J Neurosci* **29:** 10788–10801

Wood SJ, Slater CR (1997) The contribution of postsynaptic folds to the safety factor for neuromuscular transmission in rat fast- and slow-twitch muscles. *J Physiol* **500**(Part 1)**:** 165–176

Wu H, Xiong WC, Mei L (2010) To build a synapse: signaling pathways in neuromuscular junction assembly. *Development* **137:** 1017–1033

Yang G, Gong YD, Gong K, Jiang WL, Kwon E, Wang P, Zheng H, Zhang XF, Gan WB, Zhao NM (2005) Reduced synaptic vesicle density and active zone size in mice lacking amyloid precursor protein (APP) and APP-like protein 2. *Neurosci Lett* **384:** 66–71

Yao LL, Liu XY, Jin JY, Tao BB, Chen YJ, Yu YC, Bian WH, Yu J, Huang J, Wang YG (2011) Expression and ultrastructural localization of Mint2 in the spinal cord of rats. *Mol Biol Rep* **38:** 667–673

Young-Pearse TL, Chen AC, Chang R, Marquez C, Selkoe DJ (2008) Secreted APP regulates the function of full-length APP in neurite outgrowth through interaction with integrin beta1. *Neural Dev* **3:** 15

